Modeling gravitational redshifts using perturbation theory

Elena Giusarma

+ Shadab Alam (EU), Rupert Croft (CMU), Shirley Ho (CMU, LBNL, BCCP) and Hongyu Zhu (CMU)

Nordita Stockholm, July 2017

Measurements and Special Relativistic Beaming:

- S. Alam, H. Zhu, R. A. Croft, S.Ho, E. Giusarma, MNRAS (2017) 470 (3): 2822-2833.
- S. Alam, R. A. Croft, S.Ho, H. Zhu, E. Giusarma, accepted to MNRAS (2017) https://doi.org/10.1093/mnras/stx1684 **See Alam's talk!**

N-body Simulations:

- H. Zhu, S. Alam, R. A. Croft, S. Ho, E. Giusarma, accepted to MNRAS (2017) https://doi.org/10.1093/mnras/stx1644 **See Alam's talk!**

MANGA results:

- H. Zhu, R. A. Croft, A. Leauthaud, S. Alam, S. Ho, E. Giusarma, in preparation **See Croft's talk!**

Measurements and Special Relativistic Beaming:

- S. Alam, H. Zhu, R. A. Croft, S.Ho, E. Giusarma, MNRAS (2017) 470 (3): 2822-2833.
- S. Alam, R. A. Croft, S.Ho, H. Zhu, E. Giusarma, accepted to MNRAS (2017) https://doi.org/10.1093/mnras/stx1684 **See Alam's talk!**

N-body Simulations:

- H. Zhu, S. Alam, R. A. Croft, S. Ho, E. Giusarma, accepted to MNRAS (2017) https://doi.org/10.1093/mnras/stx1644 **See Alam's talk!**

MANGA results:

- H. Zhu, R. A. Croft, A. Leauthaud, S. Alam, S. Ho, E. Giusarma, in preparation **See Croft's talk!**

Theoretical approach:

- E. Giusarma, S. Alam, R. A. Croft, S. Ho and H. Zhu in preparation

Redshift distortions

In a homogeneous and isotropic Universe: light propagates in a straight light, we measure r(z).

The Universe is inhomogeneous:

- redshift is affected by peculiar velocities of galaxies,
- light is lensed by matter between the galaxies and the observer,
- the distribution of galaxies does not trace directly the distribution of dark matter (bias).

The observed positions of galaxies are shifted radially and transversally and the cross-correlation function is distorted.

Redshift distortions

- Isotropic correlation function depends only on the scalar separation: $r_{12} \equiv |\boldsymbol{r}_1 - \boldsymbol{r}_2|$

Monopole

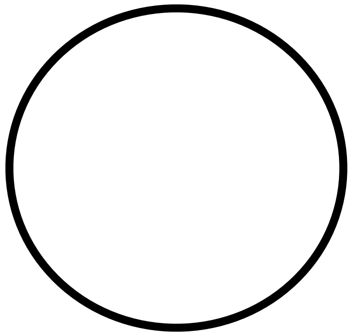

- Redshift distortions break the isotropy of the correlation function but still symmetric

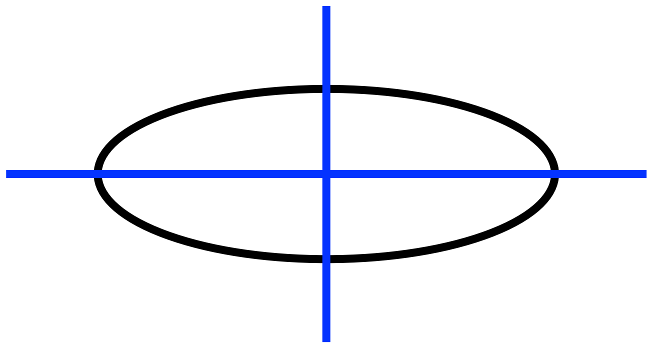

Quadrupole

$$\xi'(\sigma,\pi) = \xi_0(s)P_0(\mu) + \xi_2(s)P_2(\mu) + \xi_4(s)P_4(\mu)$$

$$\xi_0(s) = \left(1 + \frac{2\beta}{3} + \frac{\beta^2}{5}\right)\xi(r)$$

$$\xi_2(s) = \left(\frac{4\beta}{3} + \frac{4\beta^2}{7}\right)[\xi(r) - \bar{\xi}(r)]$$

$$\xi_4(s) = \frac{8\beta^2}{35}\left[\xi(r) + \frac{5}{2}\bar{\xi}(r) - \frac{7}{2}\bar{\bar{\xi}}(r)\right]$$

Legendre Polynomials

$\beta = \Omega^{0.6}/b$

Kaiser, 1987

Hamilton, 1997

Relativistic distortions

- Contribution of different effects: gravitational redshift, Doppler, special relativistic beaming, light cone effects…
- Break the symmetry of the correlation function.
- Effects are small: we need to look at large-scale structures.
- In order to isolate the relativistic effects we can study anti-symmetries in the correlation function.
- We need two populations of galaxies: faint and bright.
- They generate an odd moment namely dipole (l=1).
- We can quantify the asymmetry with the dipole!

Yoo et al. Phys. Rev. D, 86, 2012
Challinor and Lewis Phys.Rev.D84, 2011

Bonvin et al. Phys. Rev. D89 2014
Bonvin Class. Quant. Grav. 2014
Gaztanaga et al. JCAP 2017

Proposed by Einstein in the development of General Relativity

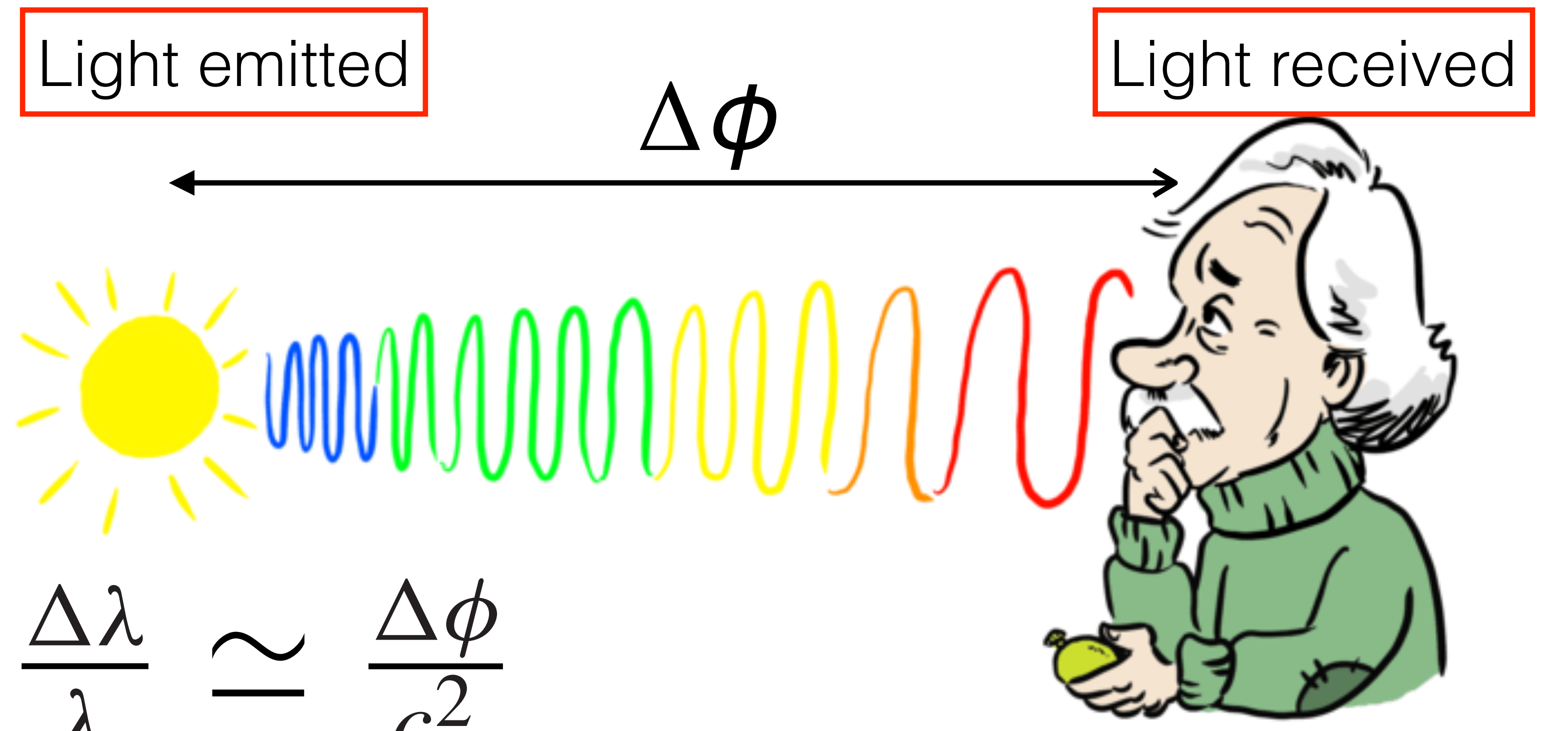

$$z_{\rm g} = \frac{\Delta\lambda}{\lambda} \simeq \frac{\Delta\phi}{c^2}$$

Redshift of galaxy: $cz = H(z)r + v_{\rm pec} + cz_{\rm g} + \ldots$

Proposed by Einstein in the development of General Relativity

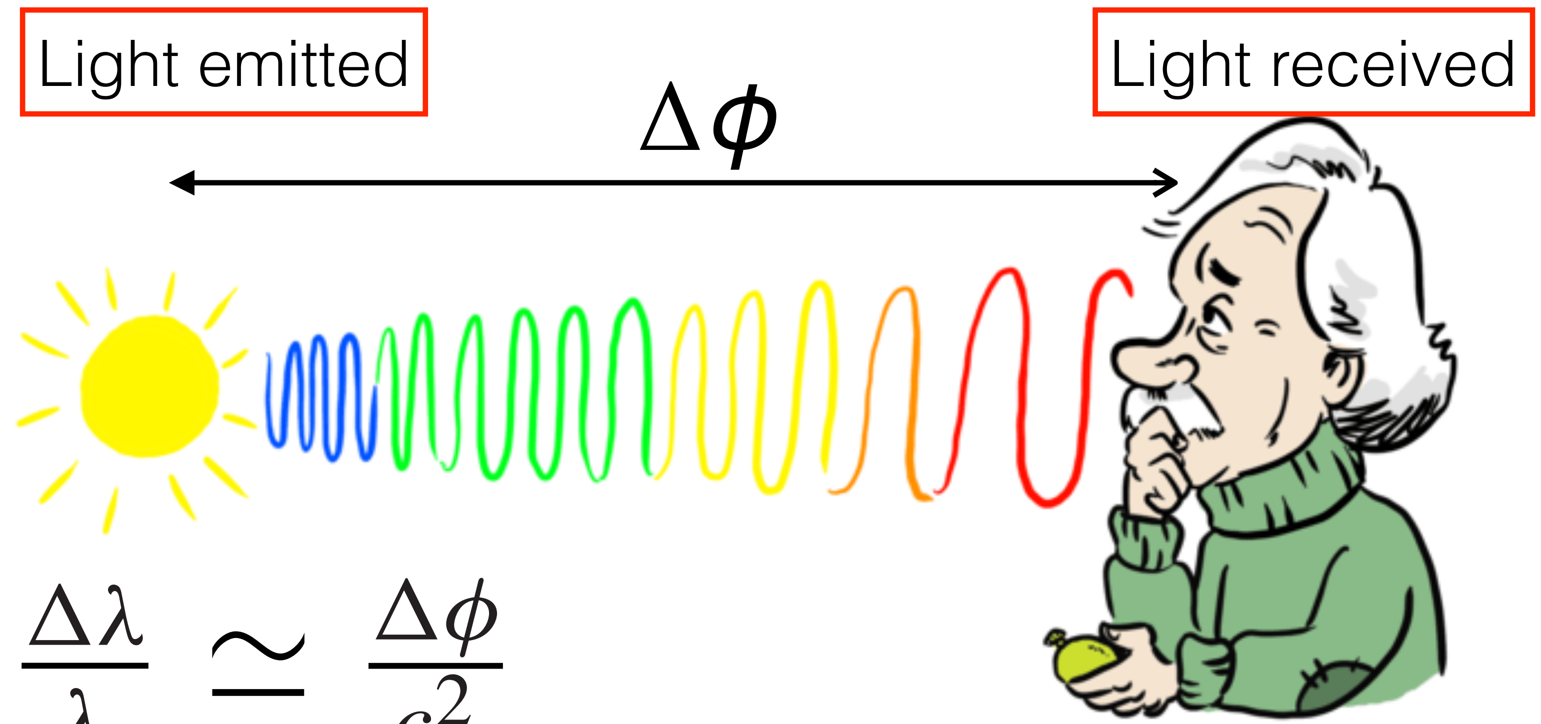

$$z_g = \frac{\Delta\lambda}{\lambda} \simeq \frac{\Delta\phi}{c^2}$$

Redshift of galaxy: $cz = H(z)r + v_{\rm pec} + cz_g + \ldots$

- General Relativity perturbation theory
- Newtonian Perturbation theory

General Relativity perturbation theory

Cross-correlation function between two galaxy populations:

$$\xi_{g1g2}(z,z') = \langle \delta_{g1}(\mathbf{x},z)\delta_{g2}(\mathbf{x}',z')\rangle \neq \xi_{g2g1}(z',z)$$

g1= bright (B) population with higher mass

g2 = faint (F) population with lower mass.

Among all the physical processes associated with galaxy properties, dynamics and environment which can lead to a non-zero dipole moment in cross-correlation function, we consider:

- Relativistic effect: $\langle \hat{\xi}_{\rm rel}(r)\rangle = (b_B - b_F)\frac{f}{2\pi^2}\left(\frac{\dot{\mathcal{H}}}{\mathcal{H}^2} + \frac{2}{\chi\mathcal{H}}\right)\frac{\mathcal{H}}{\mathcal{H}_0}\int dk k \mathcal{H}_0 P(k,\bar{z}) j_1(kr)$
- Wide-angle effect: $\langle \hat{\xi}^{\sigma}_{\rm wide}(r)\rangle = -\frac{2f}{5}(b_B - b_F)\frac{r}{\chi}\nu_2(r)$

where $f \equiv d\ln D/d\ln a$ and $\nu_\ell(r) = \frac{1}{2\pi^2}\int dk k^2 P(k,\bar{z}) j_\ell(kr)\,, \quad \ell = 0,2\,.$

Bonvin et al. Phys. Rev. D89 2014
Bonvin Class. Quant. Grav. 2014
Gaztanaga et al. JCAP 2017

Dipole contribution

Dipole contributions (relativistic and wide-angle) as a function of the comoving separation, *r* , computed at redshift z=0.57 and for different values of the bias.

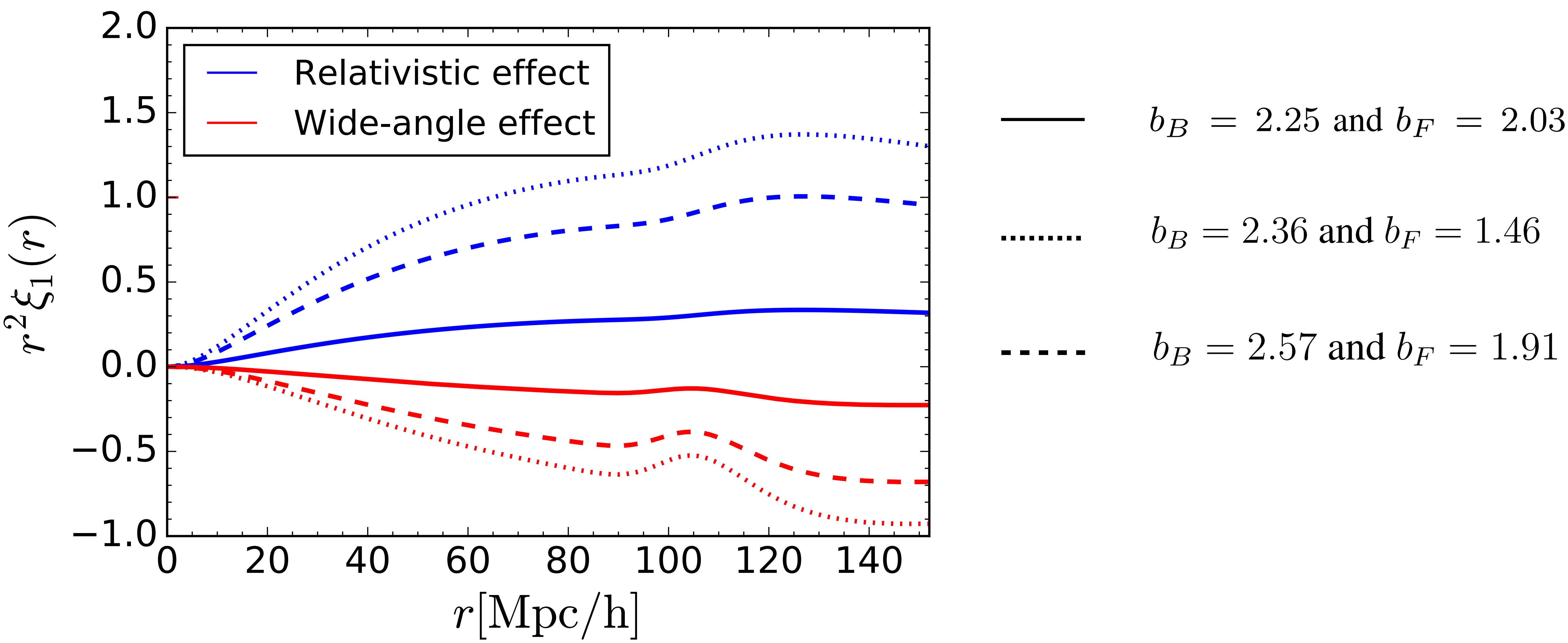

On small scales (r < 15 Mpc/h), the two contributions are canceled out. In particular a cancellation of the relativistic contribution induces no evidence for gravitational redshift effect.

EG, S. Alam, R. Croft, S. Ho, H. Zhu in preparation

Shell estimator

$$z_{\rm g}^{\rm shell}(r) = \frac{1}{3}\frac{\int_{r'}^{r'+\Delta r'} H\xi_1(r) r^3 dr'}{\int_{r'}^{r'+\Delta r'}[1+\xi_0(r)]r^2 dr}$$

R. Croft Mon. Not. Roy. Astron. Soc. 2013

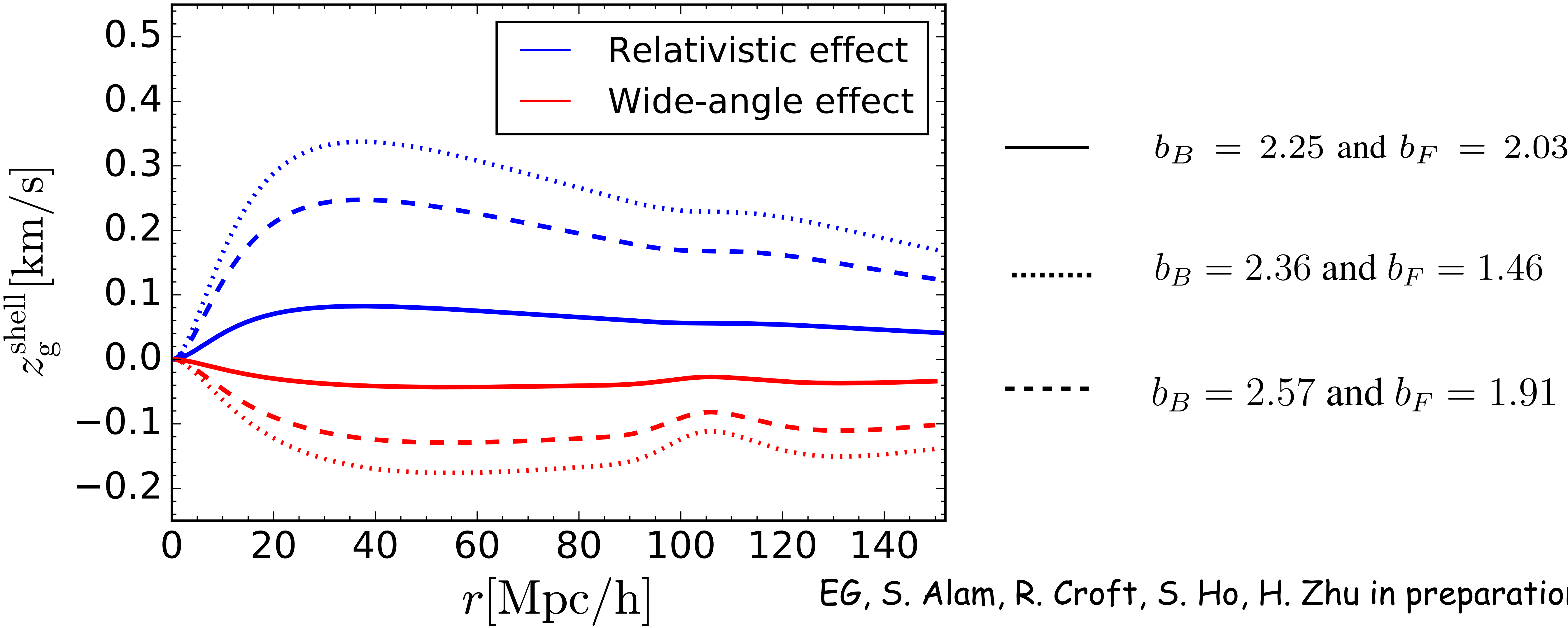

EG, S. Alam, R. Croft, S. Ho, H. Zhu in preparation

Gravitational redshift effect, included in the relativistic contribution, is cancelled out on small scales.

Shell estimator

$$z_g^{\rm shell}(r) = \frac{1}{3}\frac{\int_{r'}^{r'+\Delta r'} H\xi_1(r) r^3 dr'}{\int_{r'}^{r'+\Delta r'} [1+\xi_0(r)] r^2 dr}$$

R. Croft Mon. Not. Roy. Astron. Soc. 2013

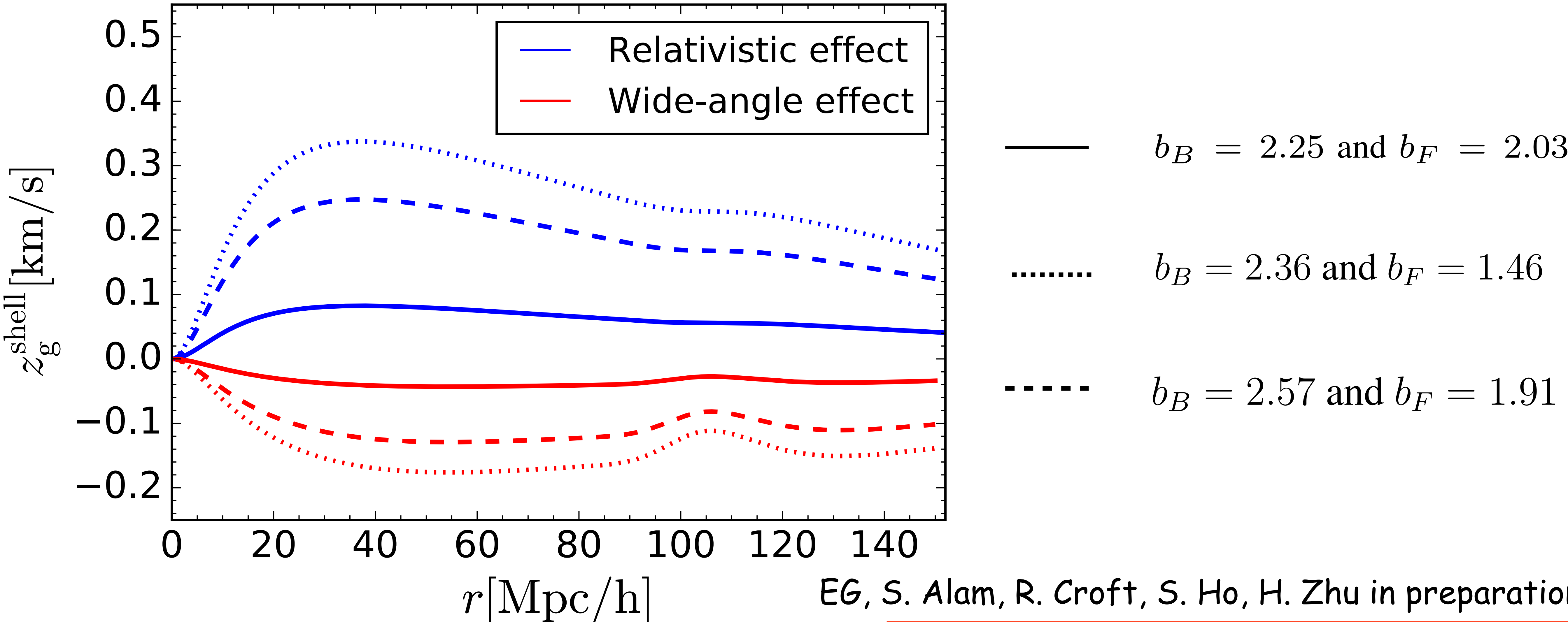

EG, S. Alam, R. Croft, S. Ho, H. Zhu in preparation

Gravitational redshift effect, included in the relativistic contribution, is cancelled out on small scales. →

General Relativity perturbation theory is able to predict relativistic and wide-angle effects on large linear scales (> 10 Mpc/h) but on small non-linear scales this approach is less accurate.

Newtonian Perturbation theory

1) Mean gravitational redshift difference between two populations of galaxies:

$$\delta z_g = z_{g1}(0) - z_{g2}(r) = \frac{G}{c}\int_{\infty}^{r} M_{12}(x)x^{-2}dx$$

R. Croft Mon. Not. Roy. Astron. Soc. 2013

We use δz_g to distort the cross-correlation function of g1 and g2 galaxies in redshift space.

2) Additional distortion due to peculiar velocities: standard linear infall for large-scale flows (Kaiser 1987) + small-scale random velocity dispersion (Davis & Peebles 1983)

$$\xi'_{g1g2}(r_\perp, r_{||}) = b_B b_F[\xi_0(s)P_0(\mu) + \xi_2(s)P_2(\mu) + \xi_4(s)P_4(\mu)]$$

$$f(v) = \frac{1}{\sigma_{12}\sqrt{2}}\exp\left(-\frac{\sqrt{2}|v|}{\sigma_{12}}\right)$$ $\longrightarrow$ Distribution function of velocities where σ_{12}=300 km/s.

$b_B = 2.25$ and $b_F = 2.03$

Redshift space cross-correlation function:

$$\xi_{g1g2}(r_\perp, r_\parallel) = \int_{\infty}^{\infty} f(v) dv \xi'_{g1g2}\left(r_\perp, r_\parallel - \frac{cz_g(r) - (1+z)v}{H(z=0.57)}\right)$$

real space

Grav. redshift x300

Pec. vel.: Kaiser +Finger of God

Combined: grav. redshift +pec. vels.

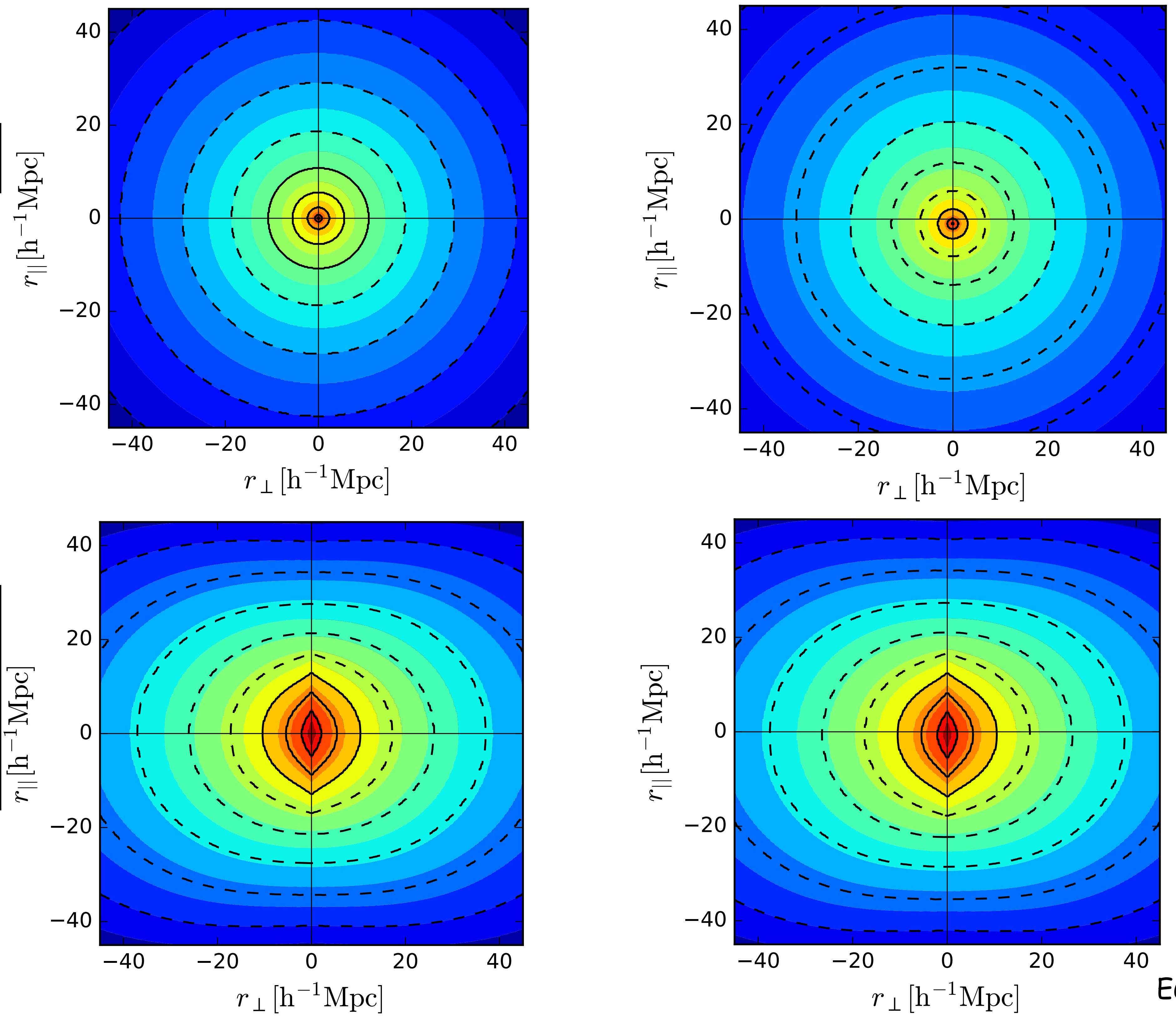

EG et al. in preparation

In order to study the dipole and shell estimator, we decompose the 2d cross-correlation functions into different moments using Legendre polynomials:

$$\xi_\ell(r) = \frac{2\ell+1}{2}\int_0^1 \xi_{g1g2}(r_\perp, r_\parallel) P_\ell(\cos\theta)\, d\cos\theta \qquad \ell = 0, 1, 2$$

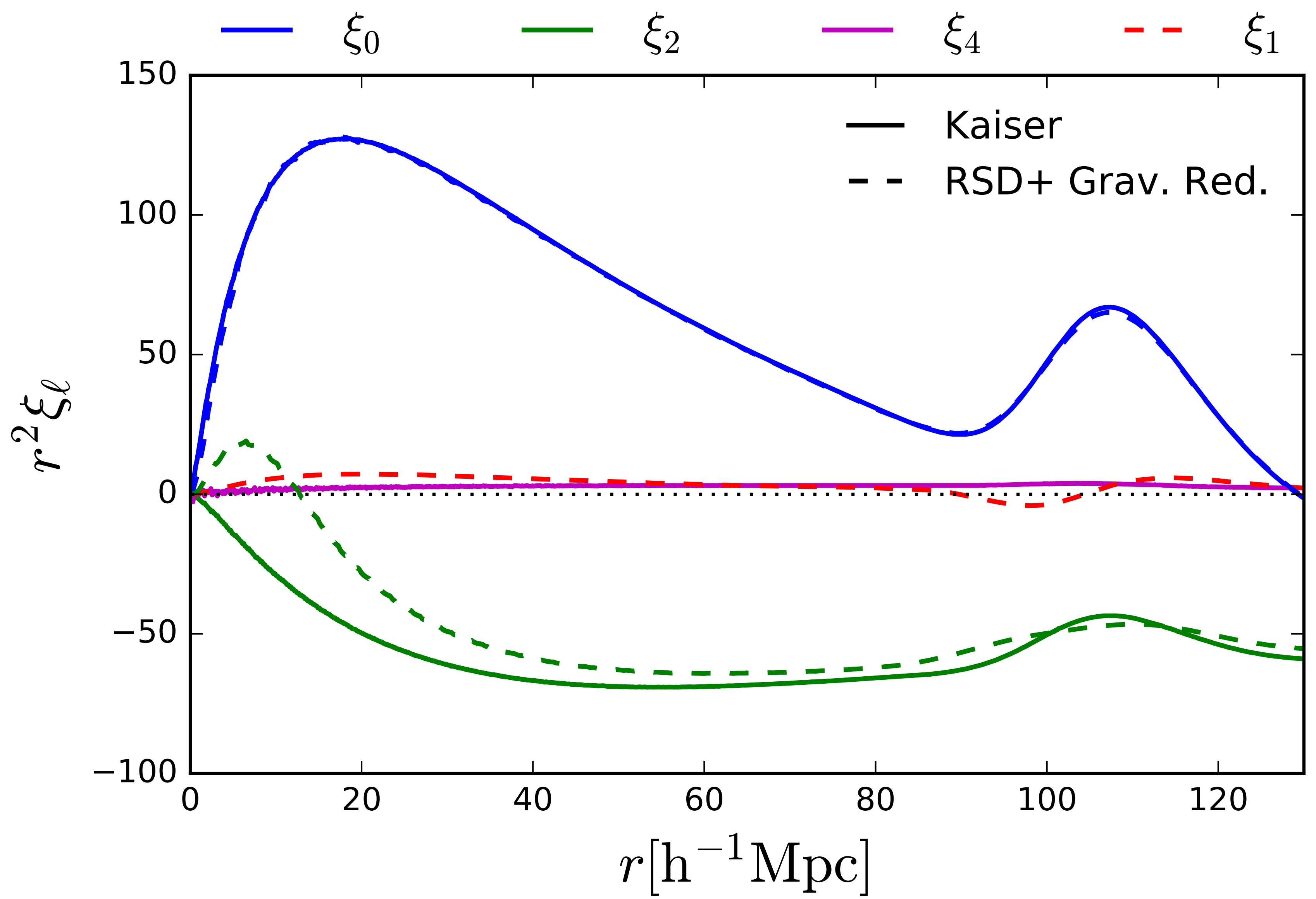

EG, S. Alam, R. Croft, S. Ho, H. Zhu in preparation

Shell estimator

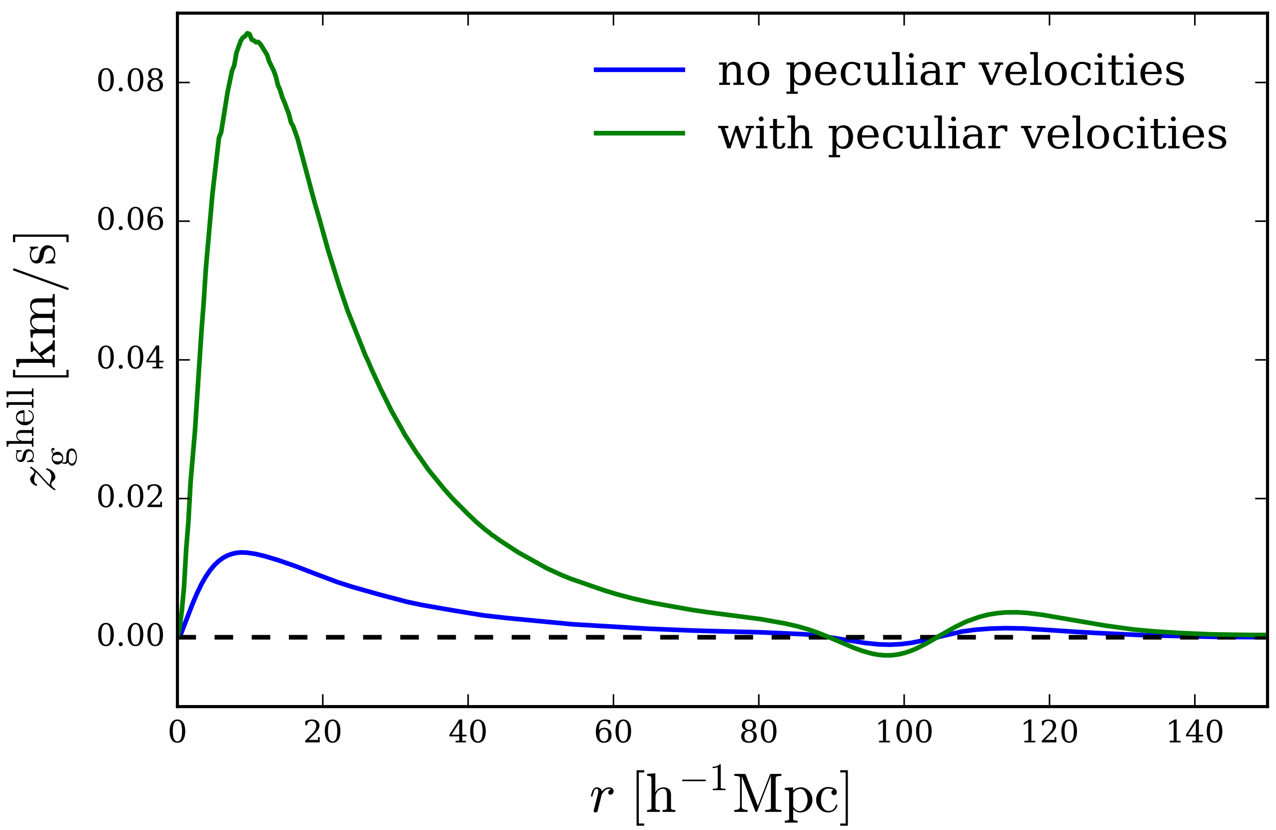

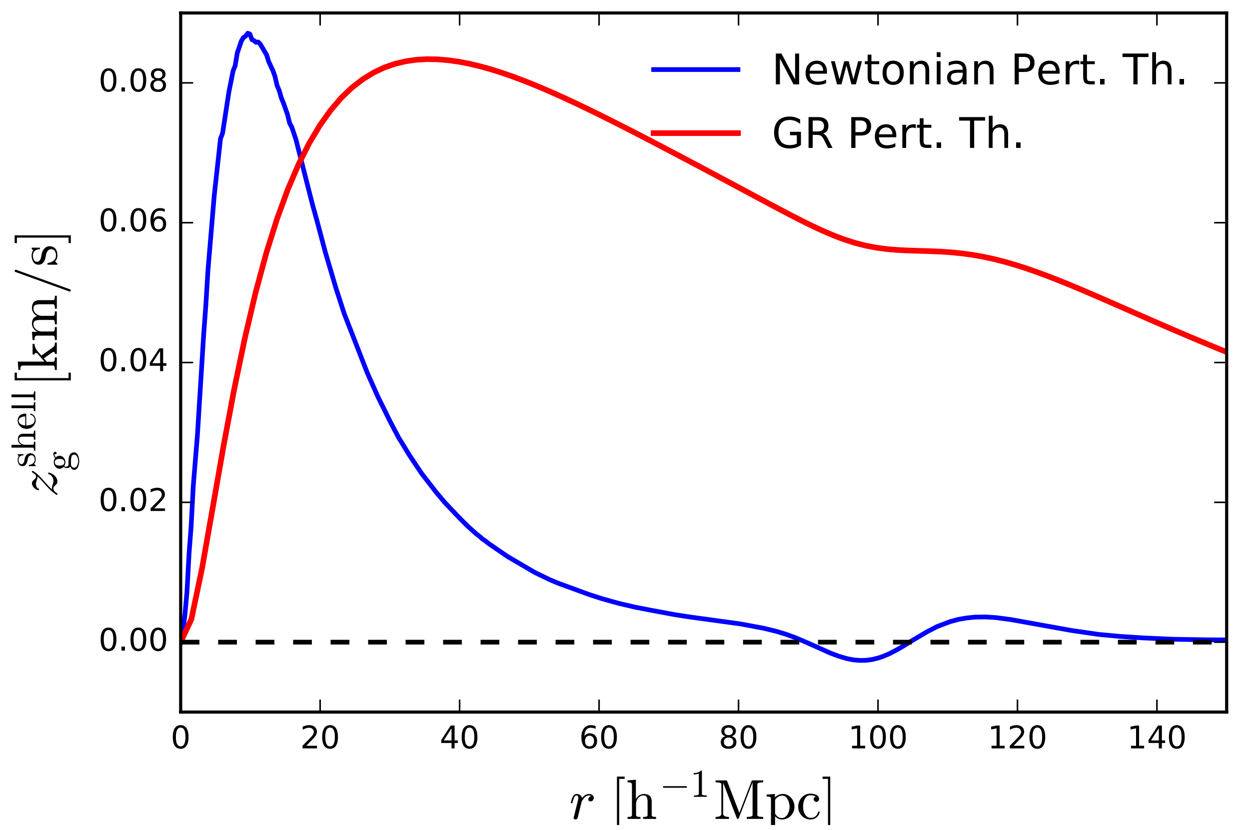

EG, S. Alam, R. Croft, S. Ho, H. Zhu in preparation

Shell estimator

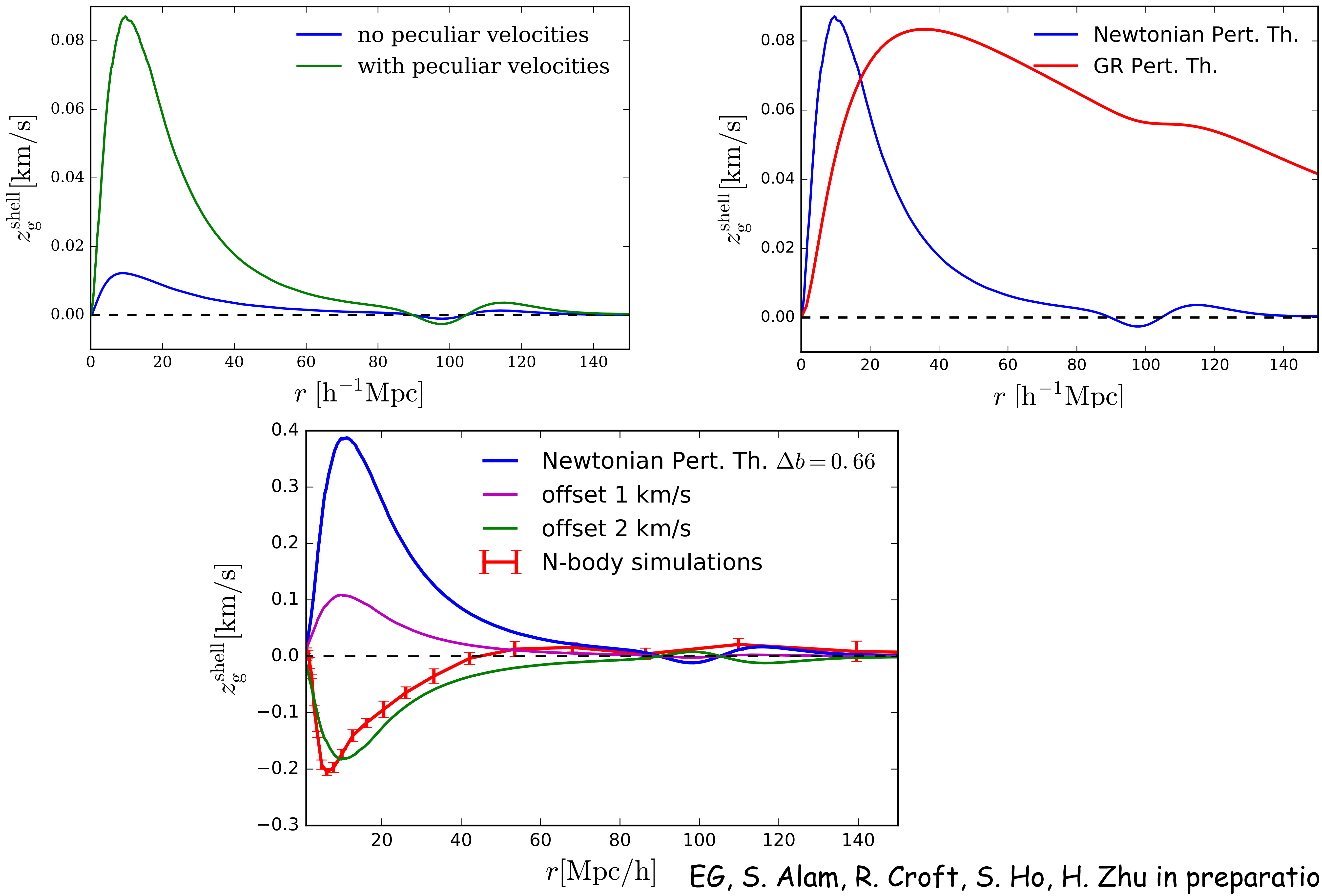

EG, S. Alam, R. Croft, S. Ho, H. Zhu in preparation

Conclusions

- ✓ Our observables are affected by relativistic effects that include gravitational redshifts.
- ✓ Relativistic effects induce asymmetries in the cross-correlation function.
- ✓ By measuring these asymmetries we can isolate the relativistic effects.
- ✓ General Relativistic perturbation theory approach makes prediction for relativistic clustering on large, linear scales.
- ✓ Newtonian perturbation theory approach makes prediction on small, non linear scales.
- ✓ There exist important uncertainties in the theoretical predictions, such as structures on galactic scales, that is necessary to model in order to explore these effects.

Thank you!

Backup

Quasi-Newtonian approach with N-body simulation to model non-linear effect at small scales.

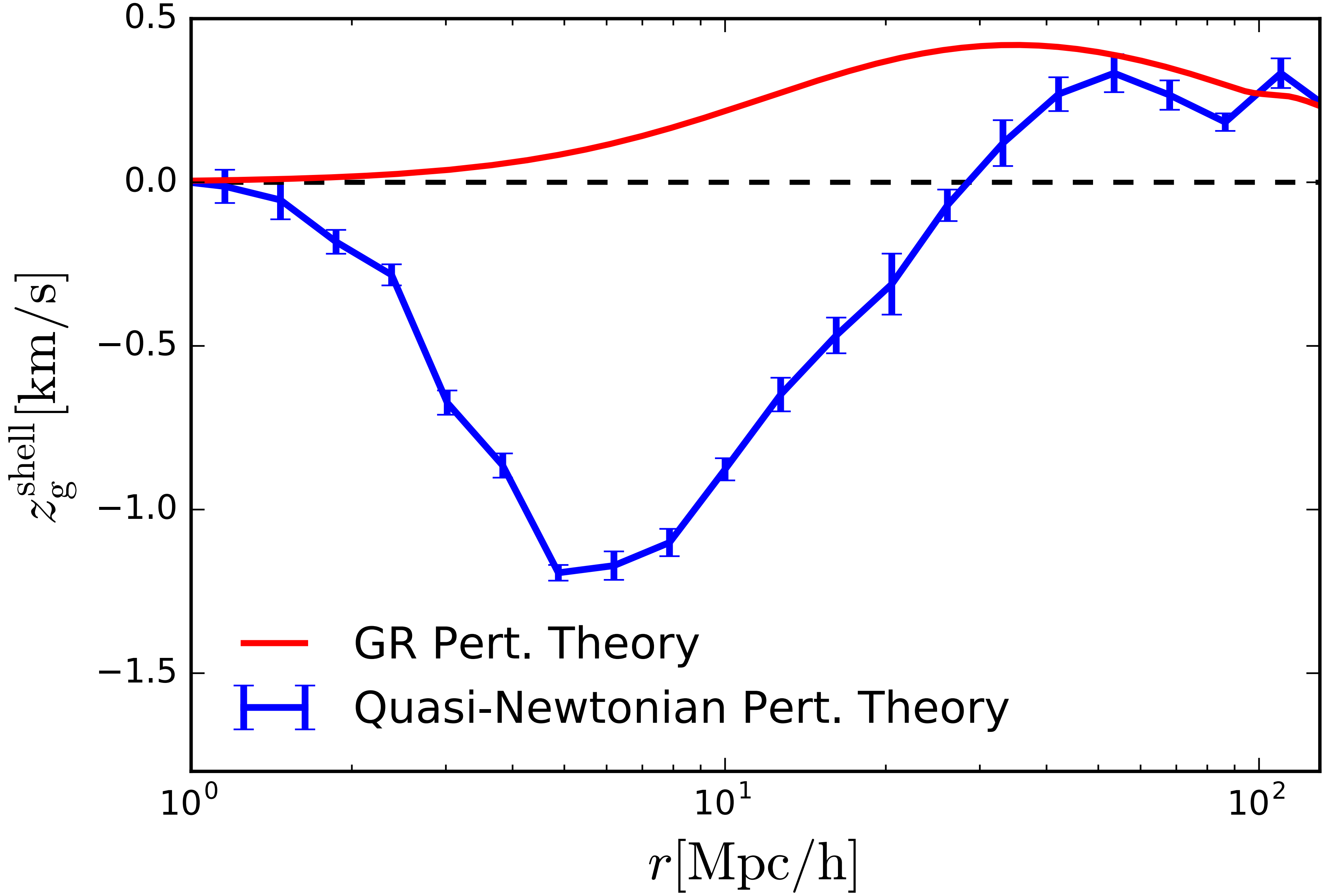

$b_B = 2.57$ and $b_F = 1.91$

Hongyu Zhu et al., MNRAS 2017

Quasi-Newtonian approach with N-body simulation to model non-linear effect at small scales.

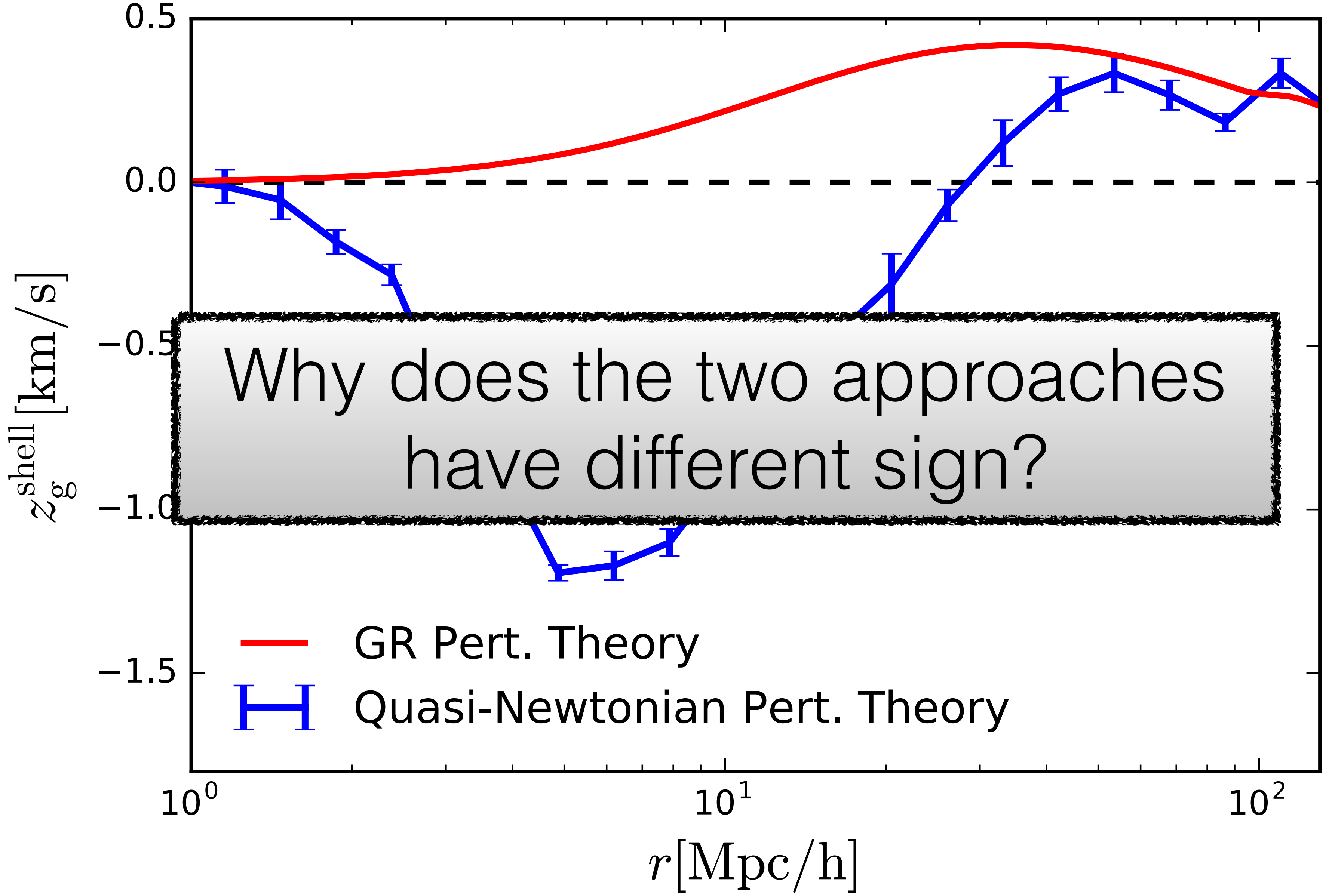

$b_B = 2.57$ and $b_F = 1.91$

Hongyu Zhu et al., MNRAS 2017

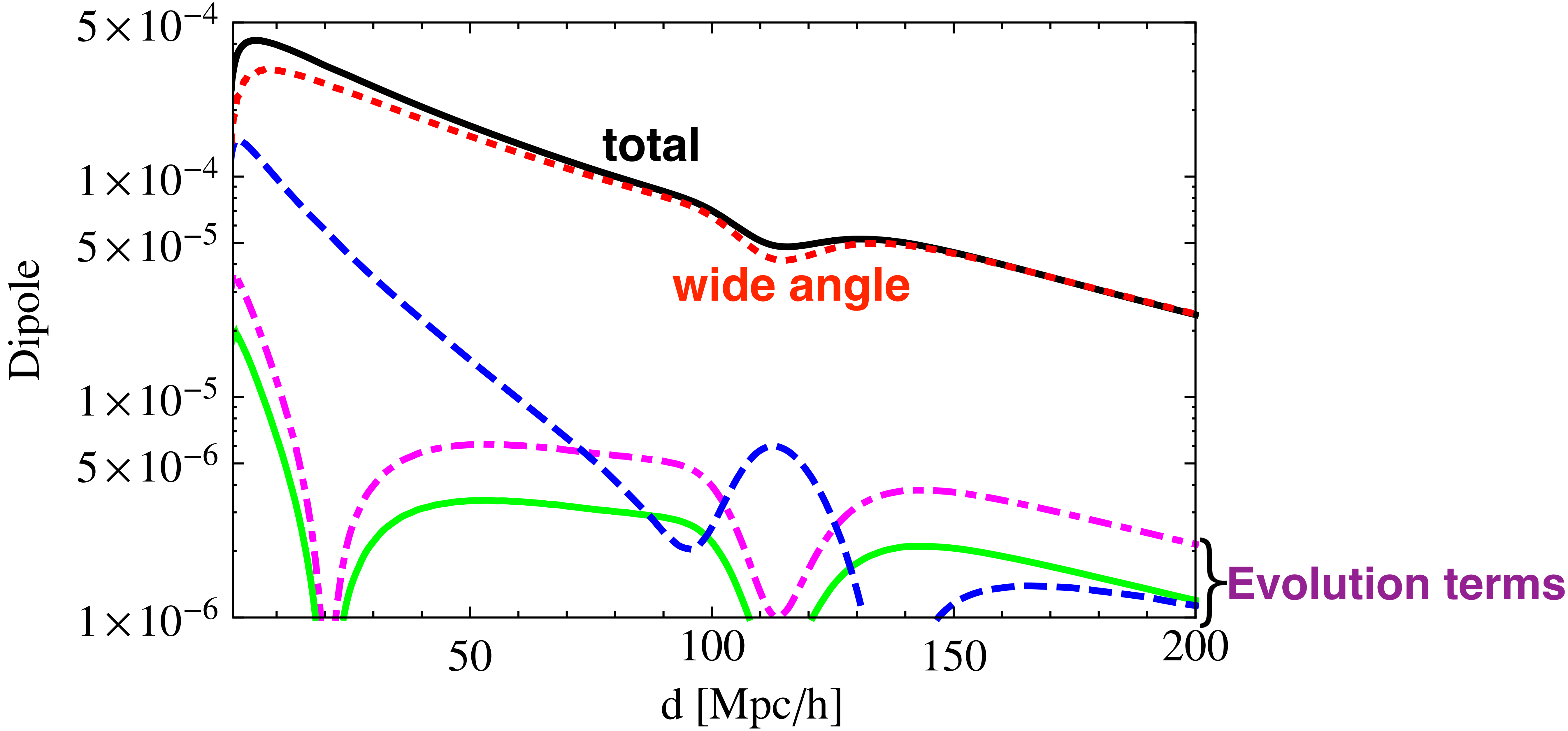

Bonvin et al. Phys. Rev. D89 2014

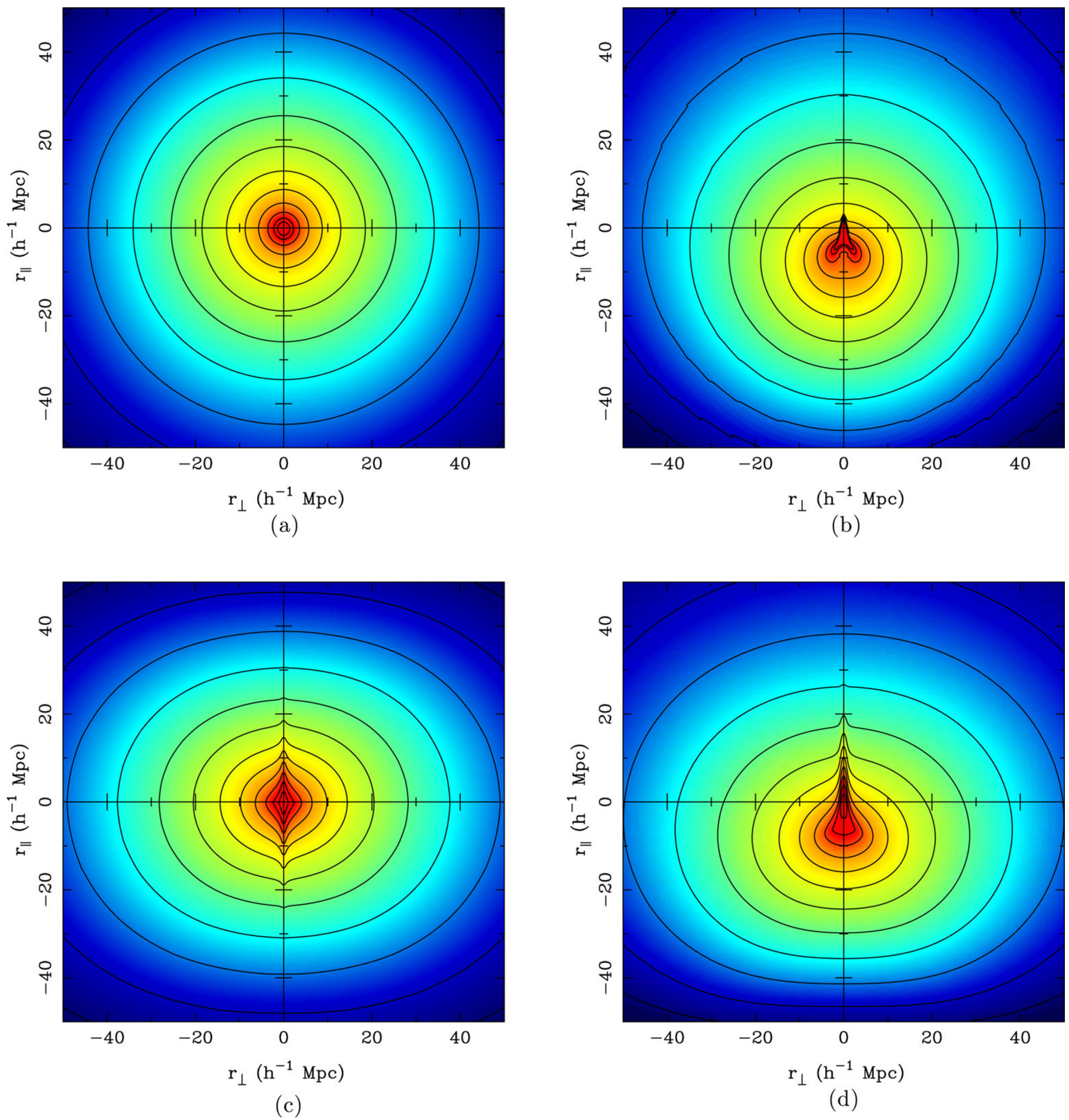

r∥ (h−1 Mpc)
r⊥ (h−1 Mpc)
−40
−20
0
20
40
(a)
(b)
(c)
(d)

N-body simulation

We consider two galaxy populations with different mean halo: *g1* high mass subset, *g2* low mass subset

Cross-correlation function g1 and g2 galaxy samples, as a function of separation parallel and perpendicular to the line of sight.

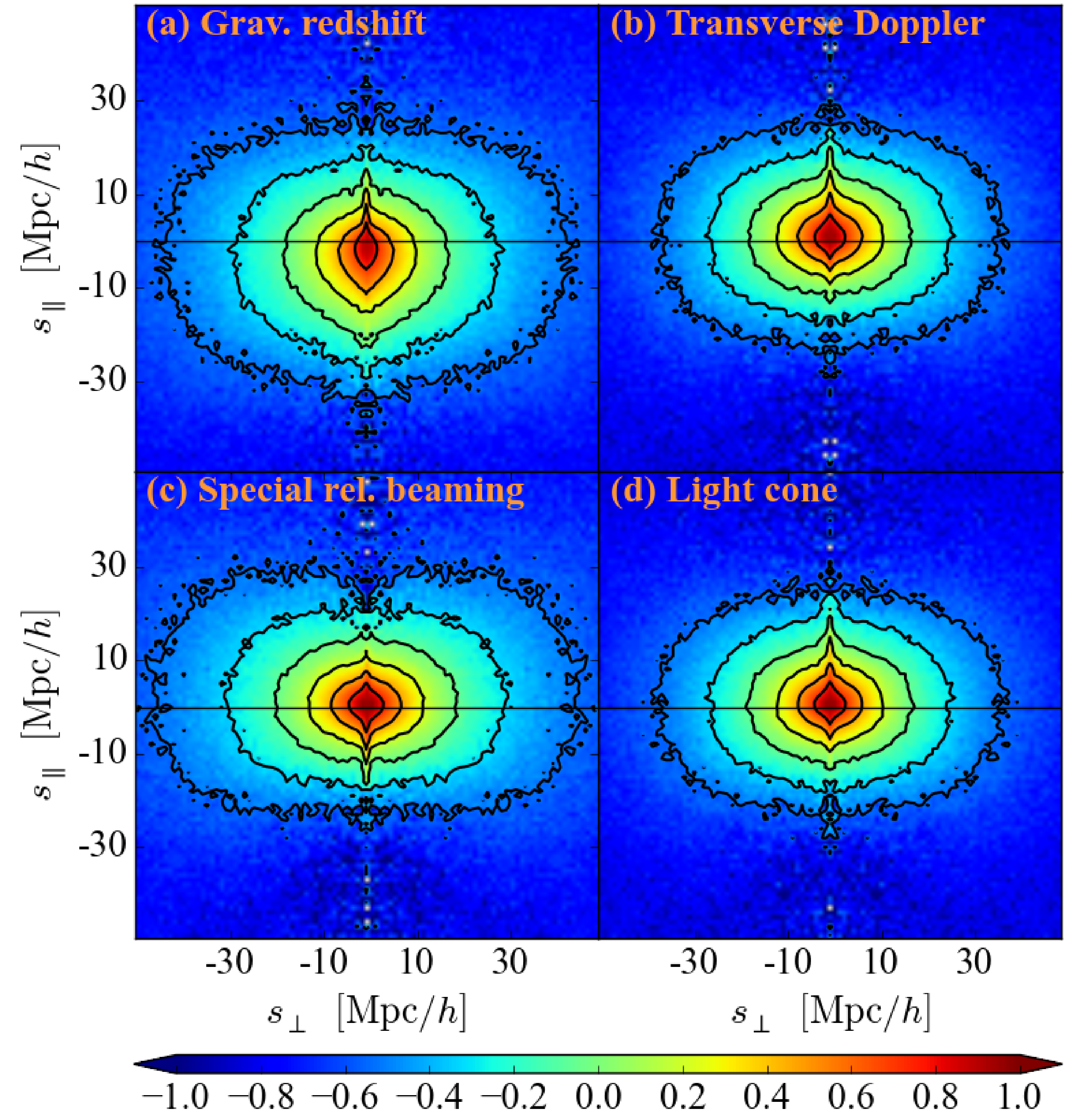

Hongyu Zhu et al., MNRAS 2017

N-body simulation

Shell estimator :

$$z_g^{shell}(s) = \frac{\int_{\theta=0}^{\theta=\pi} H s_{\parallel}[1+\xi(s,\theta)]d\theta}{\int_{\theta=0}^{\theta=\pi}[1+\xi(s,\theta)]d\theta}$$

z_g dominant effect for r<20 Mpc/h

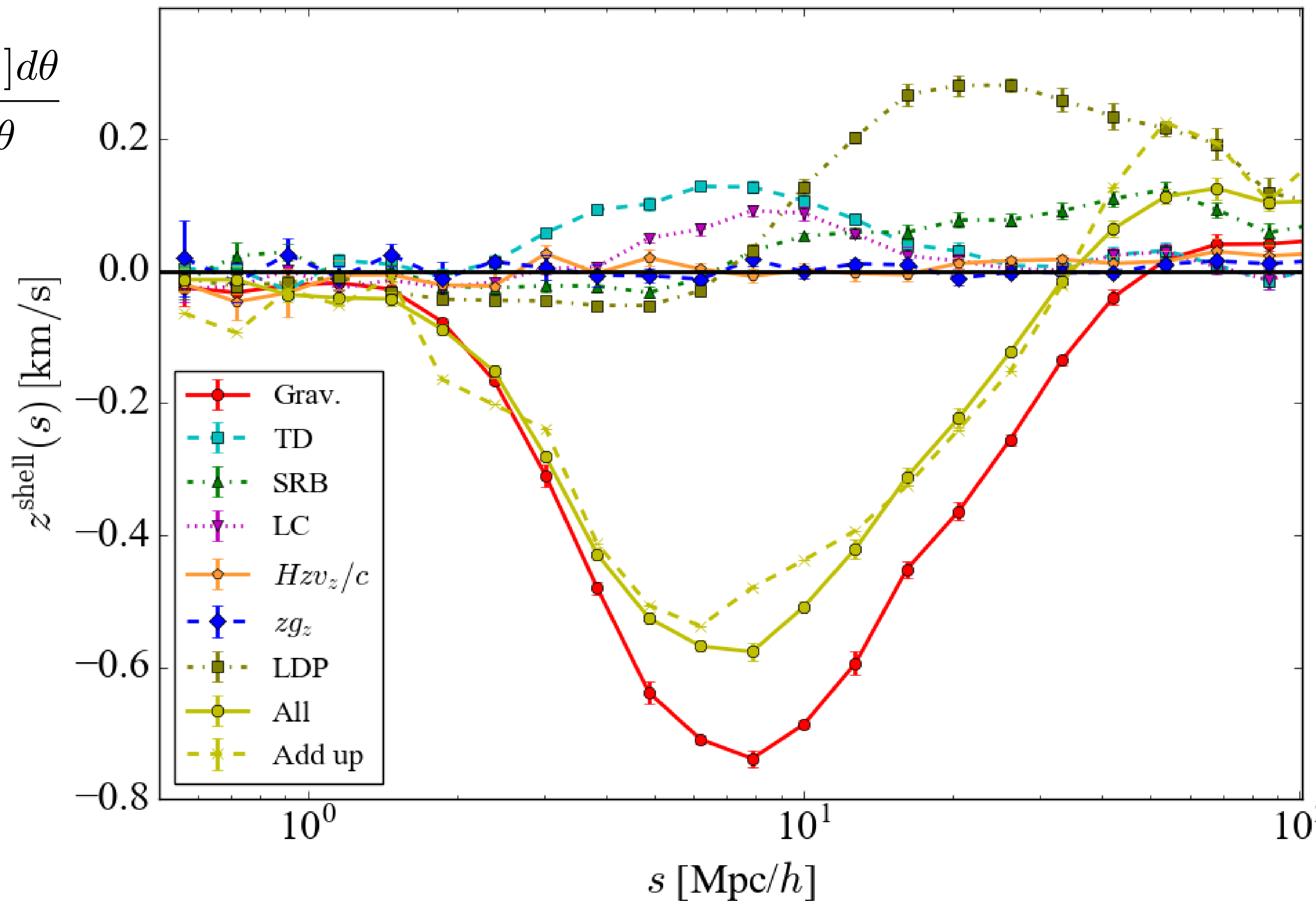

Hongyu Zhu et al., MNRAS 2017

From measurements

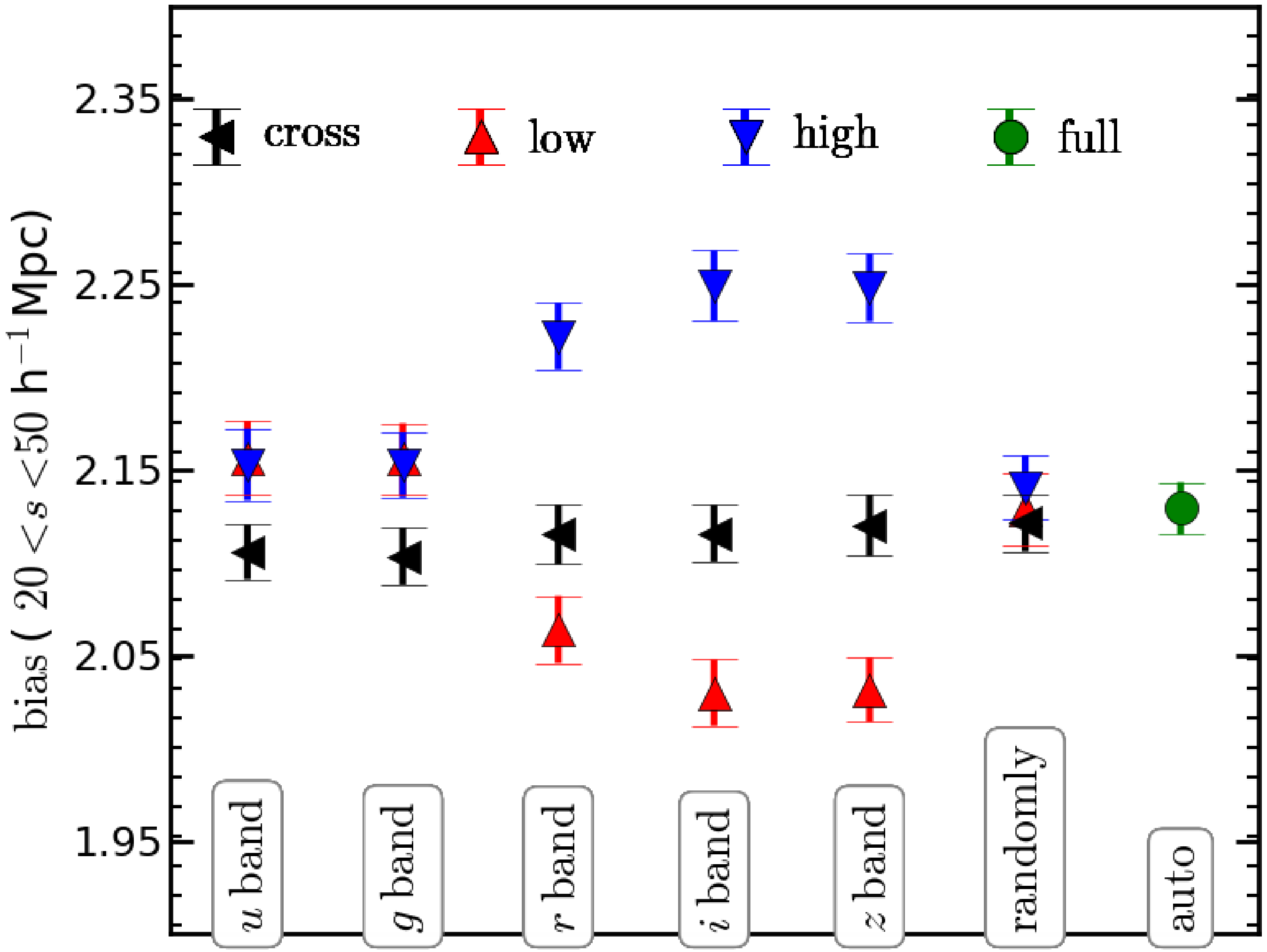

Figure 5. The bias measured for each of the sub-samples used in our analysis using scales between 20 and 50 h^{-1}Mpc. The red, blue, black and green points represent bias of low-mass auto-correlation, high-mass auto-correlation, low-high cross-correlation and full sample auto-correlation functions, respectively. The subsamples are defined by each of the five photometric magnitudes (u, g, r, i, z) and also a random split. The r, i and z samples show significantly different biases for low and high mass subsamples.

From measurements

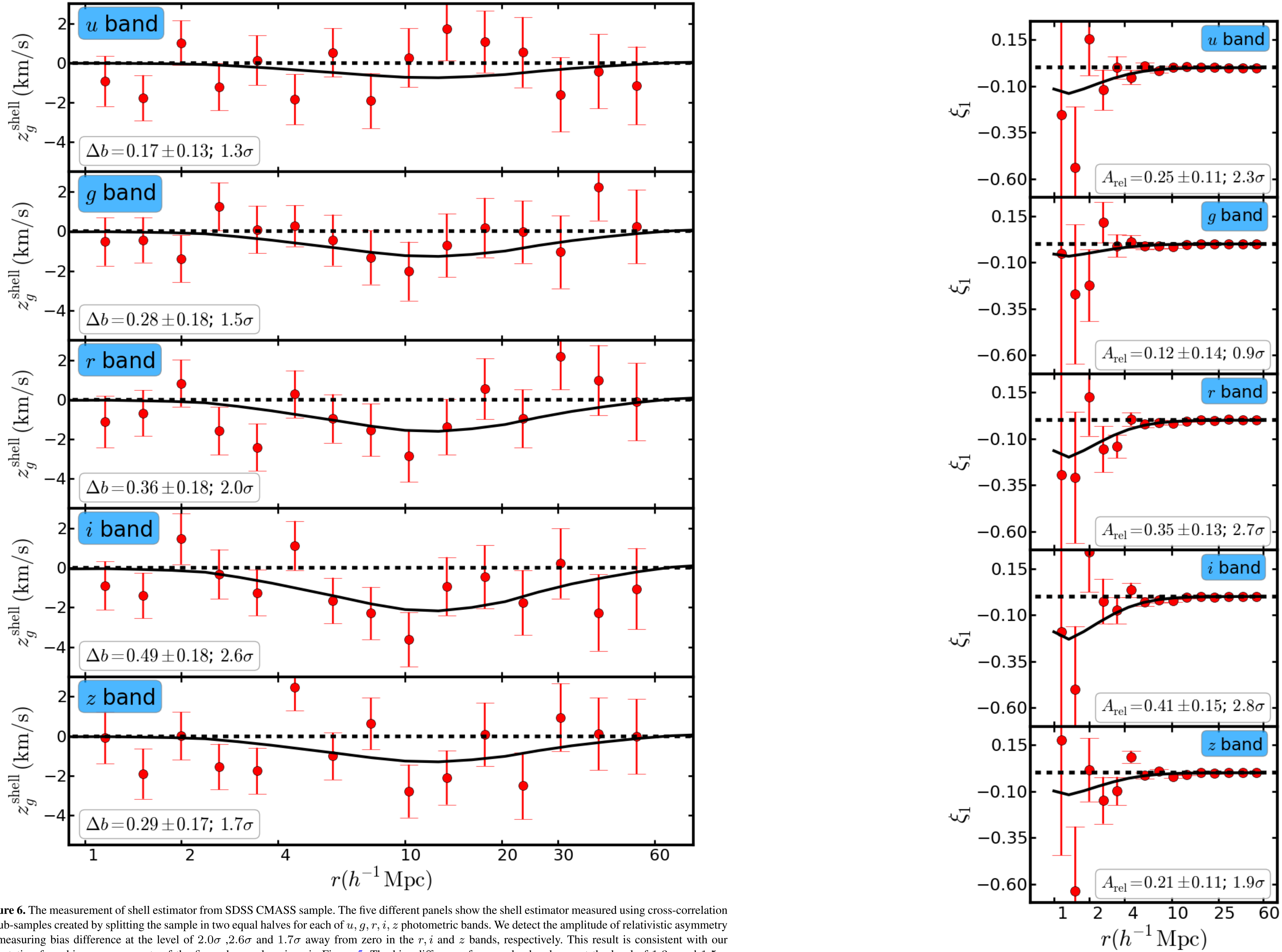

Figure 6. The measurement of shell estimator from SDSS CMASS sample. The five different panels show the shell estimator measured using cross-correlation of sub-samples created by splitting the sample in two equal halves for each of u, g, r, i, z photometric bands. We detect the amplitude of relativistic asymmetry by measuring bias difference at the level of 2.0σ ,2.6σ and 1.7σ away from zero in the r, i and z bands, respectively. This result is consistent with our expectation from bias measurements of the five sub-samples given in Figure 5. The bias difference for u and g bands are at the level of 1.3σ and 1.5σ, consistent with the expectation from biases.

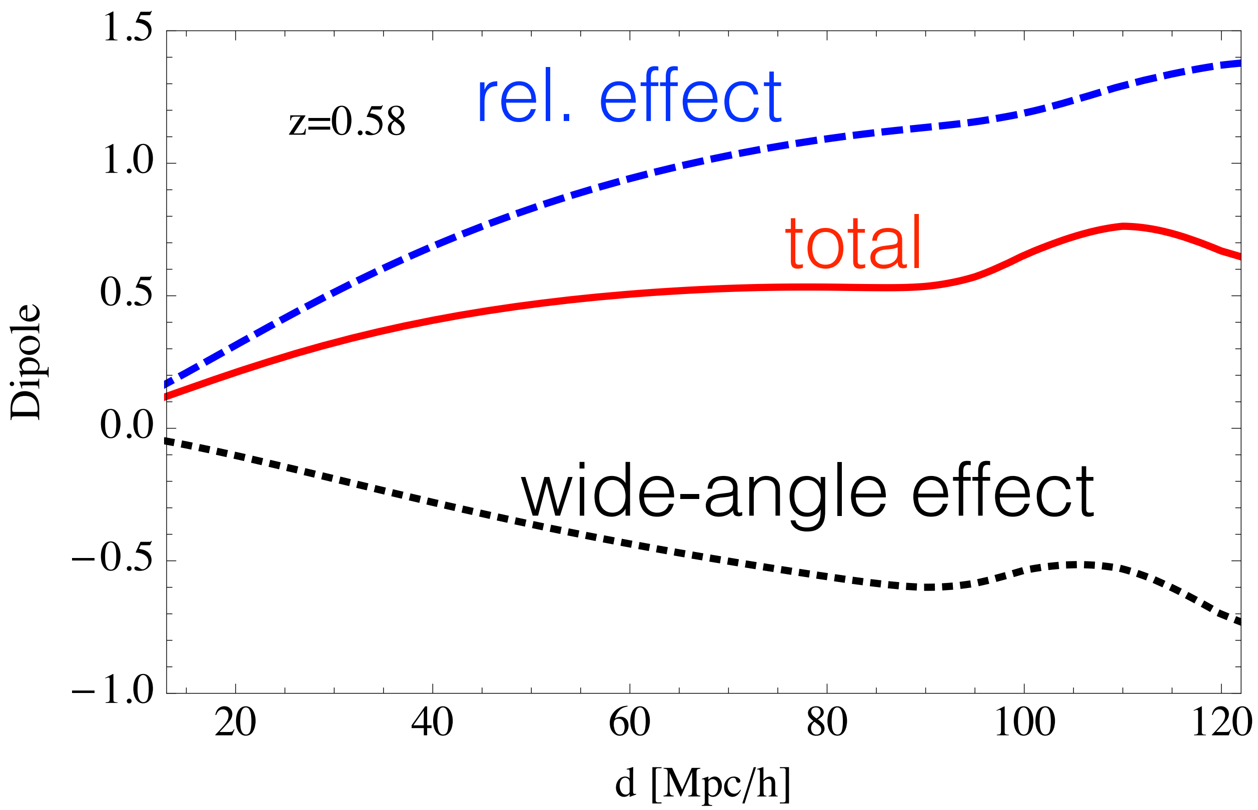

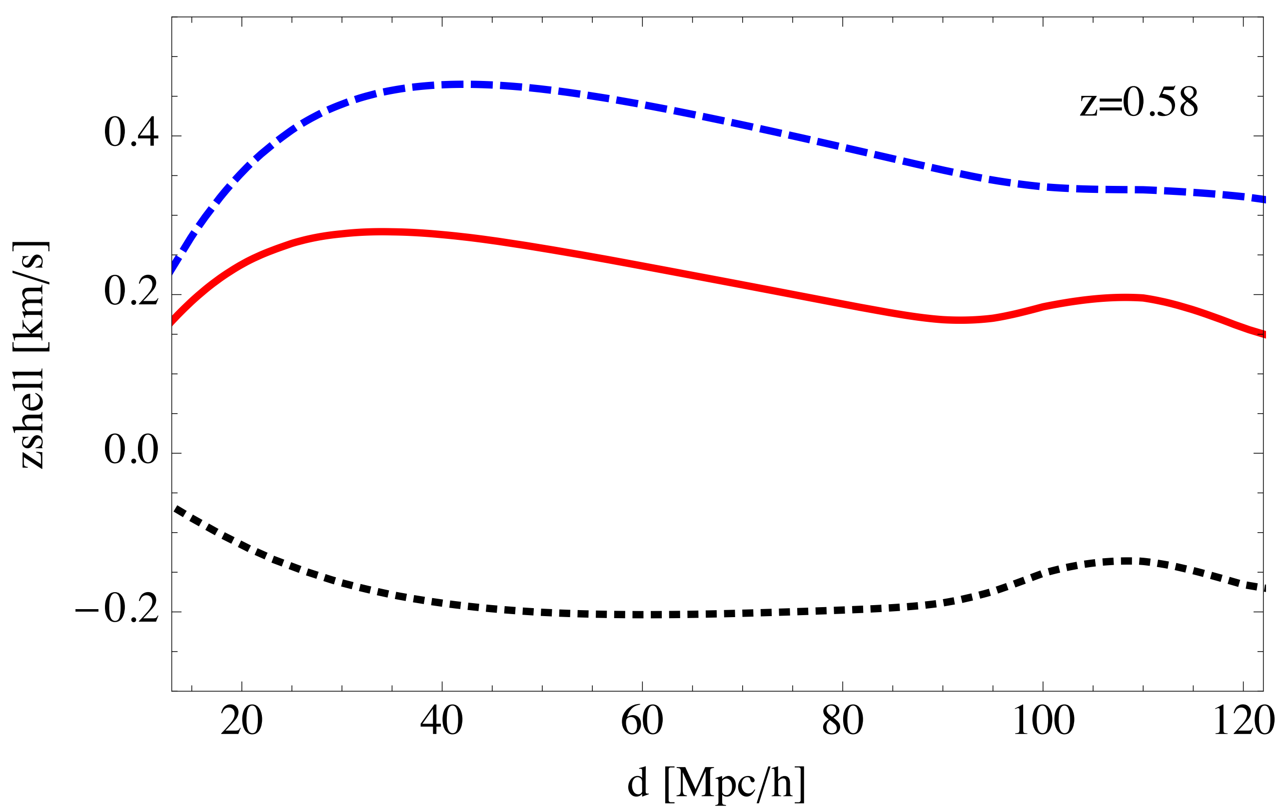

Gaztanaga et al. 2015

Observed over-density of galaxies

density

redshift space distortion

lensing

gravitational redshift

Doppler

$$
\begin{aligned}
\Delta(z,\mathbf{n}) = {} & b\cdot\delta - \frac{1}{\mathcal{H}}\partial_r(\mathbf{V}\cdot\mathbf{n}) \\
& - \int_0^r dr'\frac{r-r'}{rr'}\Delta_\Omega(\Phi+\Psi) \\
& + \left(1-\frac{\dot{\mathcal{H}}}{\mathcal{H}^2}-\frac{2}{r\mathcal{H}}\right)\mathbf{V}\cdot\mathbf{n} + \frac{1}{\mathcal{H}}\dot{\mathbf{V}}\cdot\mathbf{n} + \frac{1}{\mathcal{H}}\partial_r\Psi \\
& + \Psi - 2\Phi + \frac{1}{\mathcal{H}}\dot{\Phi} - 3\frac{\mathcal{H}}{k}V + \frac{2}{r}\int_0^r dr'(\Phi+\Psi) \\
& + \left(\frac{\dot{\mathcal{H}}}{\mathcal{H}^2}+\frac{2}{r\mathcal{H}}\right)\left[\Psi + \int_0^r dr'(\dot{\Phi}+\dot{\Psi})\right]
\end{aligned}
$$

→ potential

$$\Delta_{\mathrm{rel}} = \frac{1}{\mathcal{H}}\dot{\mathbf{V}} \cdot \hat{\mathbf{n}} + \left(1 - \frac{\dot{\mathcal{H}}}{\mathcal{H}^2} - \frac{2}{r\mathcal{H}}\right)\mathbf{V} \cdot \hat{\mathbf{n}} + \frac{1}{\mathcal{H}}\partial_r \Psi$$

$$\xi(s, \beta) = D_1^2\, f\, \frac{\mathcal{H}}{\mathcal{H}_0}\left(\frac{\dot{\mathcal{H}}}{\mathcal{H}^2} + \frac{2}{r\mathcal{H}}\right)(b_{\mathrm{B}} - b_{\mathrm{F}})\nu_1(s) \cdot \cos(\beta)$$

$$\nu_1(s) = \frac{A}{2\pi^2}\int \frac{dk}{k}\left(\frac{k}{H_0}\right)^{n_s - 1} T_\delta(k) T_\Psi(k)\, j_1(k \cdot s)$$

$$\xi_1(s) = \frac{3}{2}\int_{-1}^{1} d\mu\ \xi(s, \mu) \cdot \mu \qquad \mu = \cos\beta$$

- Gravitational Redshift of photons emitted in a gravitational potential and observed at infinity

$$z_{\rm g} = \frac{\Delta\lambda}{\lambda} \simeq \frac{\Delta\phi}{c^2}$$

- Redshift of galaxy:

$$cz = H(z)r + v_{\rm pec} + cz_{\rm g}$$

- Cappi (1995): In the massive clusters, the central galaxy is expected to have a gravitational redshift of a few tens of km/s with respect to other cluster members .

- Kim & Croft (2004): Gravitational redshifts of galaxies are statistically detectable from the survey.

- Wojtak et al. (2011) detected the gravitational redshifts in galaxy clusters using 7800 clusters in data from the SDSS survey.

- Croft (2013) proposed an estimator to measure the line-of-sight asymmetry using the cross-correlation function of the two different samples.

- Zhao et al. (2013) and Kaiser (2013) studied other important effects such as transverse Doppler effect, light cone bias and special relativistic beaming effect.

- Bonvin et al. (2014): Gravitational redshift distortion is related to the full general relativistic asymmetry of the cross-correlation of two populations of galaxies.

- Gaztanaga et al. (2015) measured the cross-correlation dipole in BOSS LOWz and CMASS samples, data release DR10 on large scales (r>20 Mpc/h).